Large area continuous position sensitive diamond detector tests

Mircea Ciobanu, ISS-Bucharest

www.spacescience.ro

3rd ADAMAS Workshop

18 – 20 November 2014

European Center for Theoretical Studies, Trento

Outline

1. Our PSDD history
2. Recent tests
   - Tests with alpha
   - Tests in microbeam
3. Improved configuration
4. Summary and outlook

History: The first sc PSDD, 2009

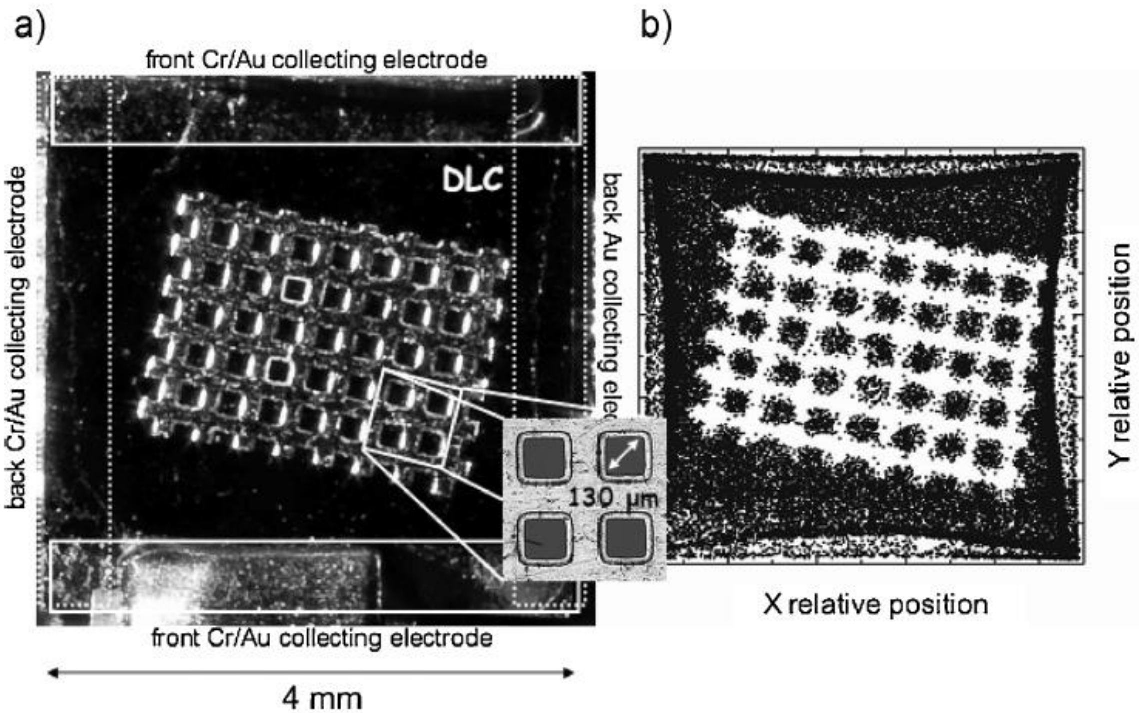

Figure 5 Preliminary results as obtained with a 2D duo-lateral scCVD-PSD. (a) A macro-photograph of the device with a masking metal grid placed on the top of the DLC entrance electrode. (b) The corresponding scatter plot measured with the device and four charge-sensitive amplifiers.

M. Pomorski, M. Ciobanu, C. Mer, M. Rebisz-Pomorska, D. Tromson and P. Bergonzo
Position-sensitive radiation detectors made of single crystal CVD diamond
Phys. Status Solidi A, 1-6 (2009) / DOI 10.1002/pssa.200982229

History: The first pc PSDD for heavy ions, 2012

position sensitive detector dimensions and FEE

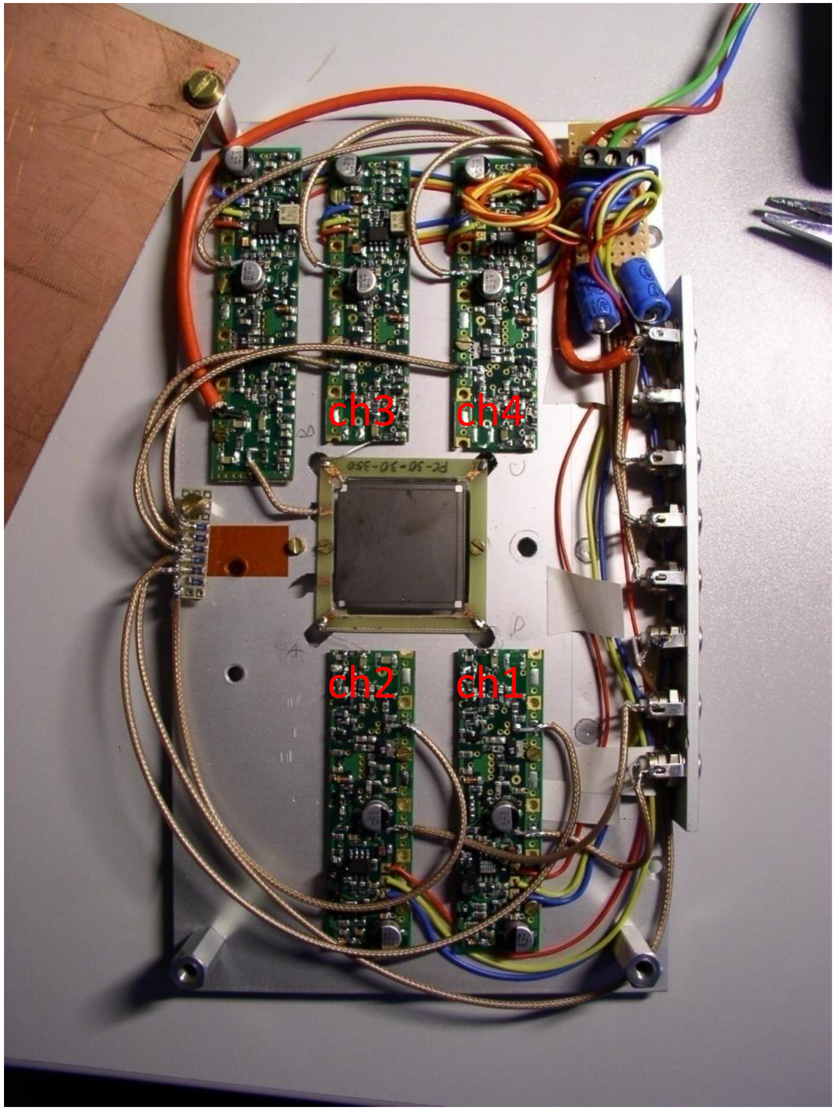

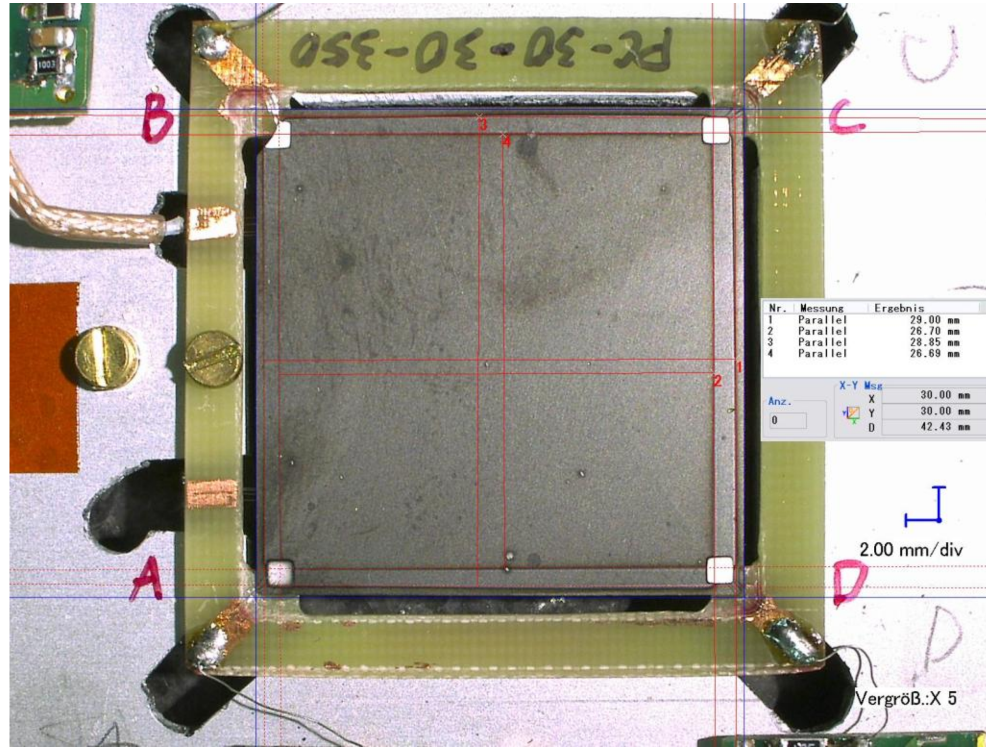

PSD diamond detector

- diamond size: 30.0mm x 30.0mm
- sensitive area: 29.0mm x 29.0mm
- resistive layer: 26.7mm x 26.7mm

M.Ciobanu, Large Area Continuous Position Sensitive Diamond Detector: First tests, 1st ADAMAS Collaboration Meeting ,16 – 18 December 2012,GSI-Darmstadt

History: First tests, 2012

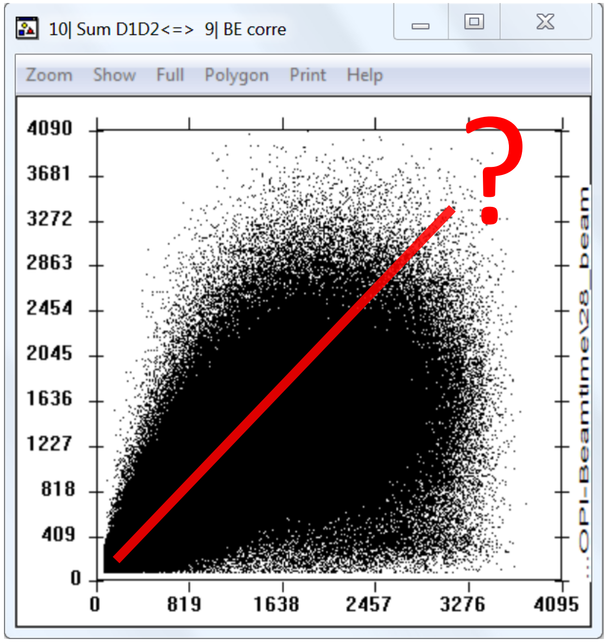

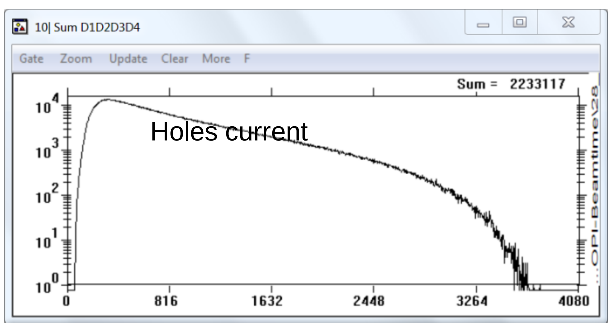

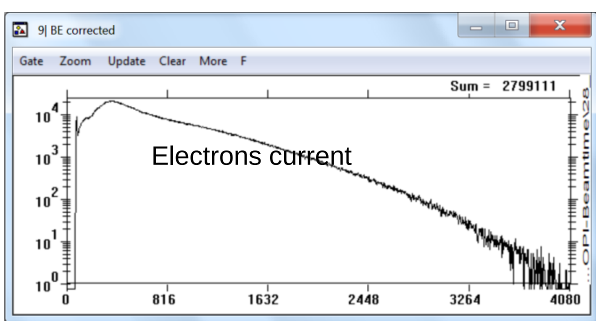

In beam (Ni-58 @ 1.7GeV/A) results

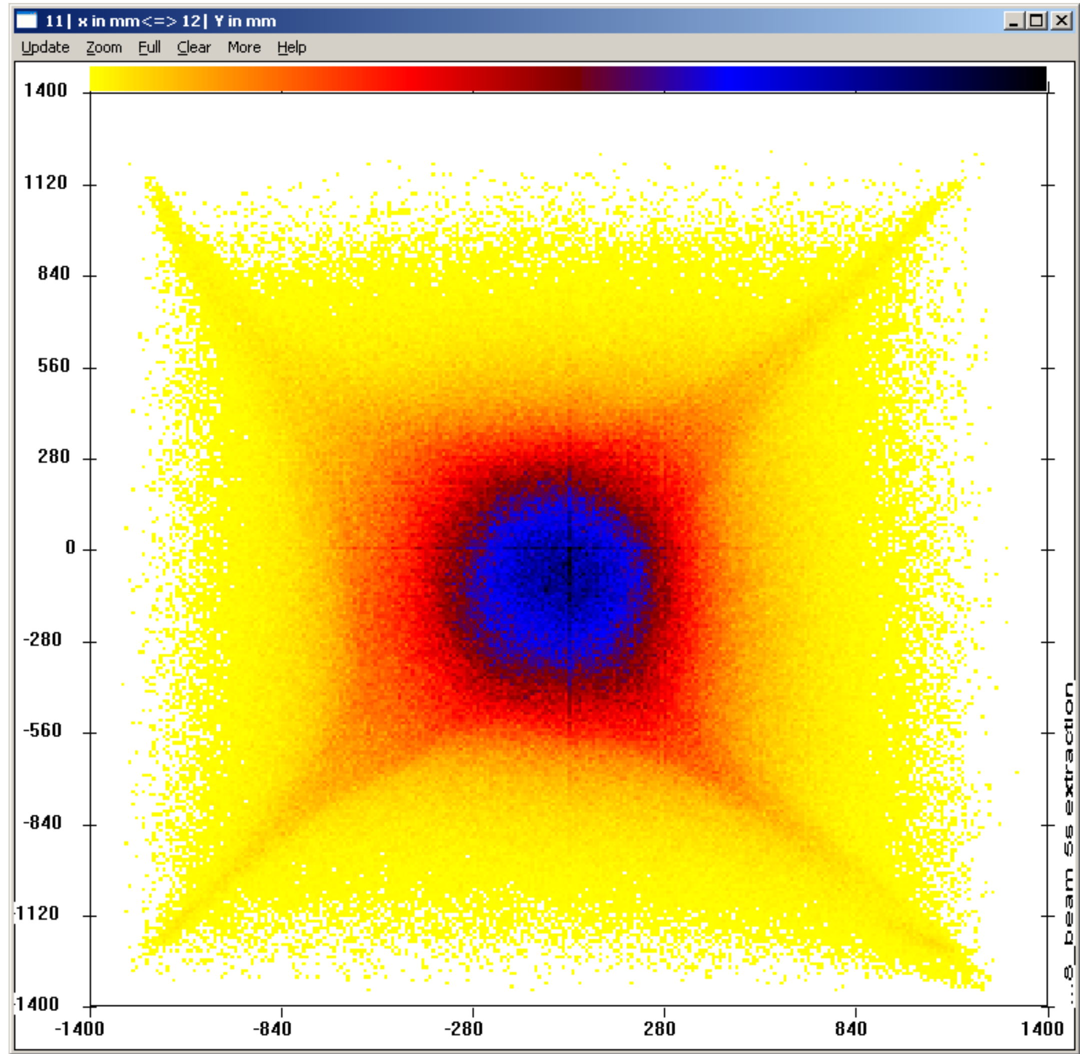

M.Ciobanu, Large Area Continuous Position Sensitive Diamond Detector: First tests, 1st ADAMAS Collaboration Meeting ,16 – 18 December 2012,GSI-Darmstadt

Recent tests: DD1

LACPSDD polycrystalline-Element 6: electronic grade, **20 mm x 20 mm**, =180µm, 2 DLC layers **(Dr. Michal Pomorski)**, electrodes and bonding (**GSI**)

substrate side

RD=29 - 35 KΩ□
growth side: strip-strip R=29.5kOhm
substrate side: strip-strip R=34.7kOhm
CD= 101pF

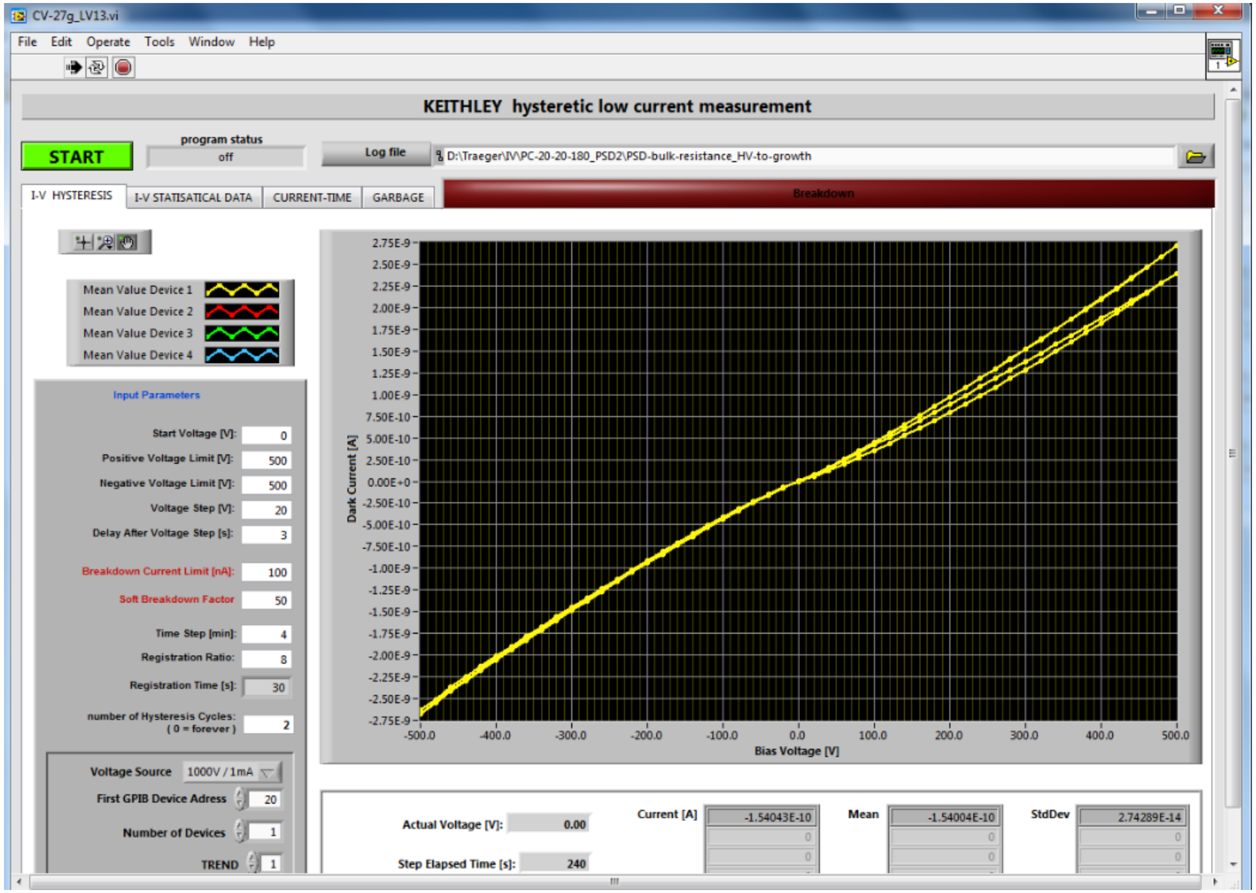

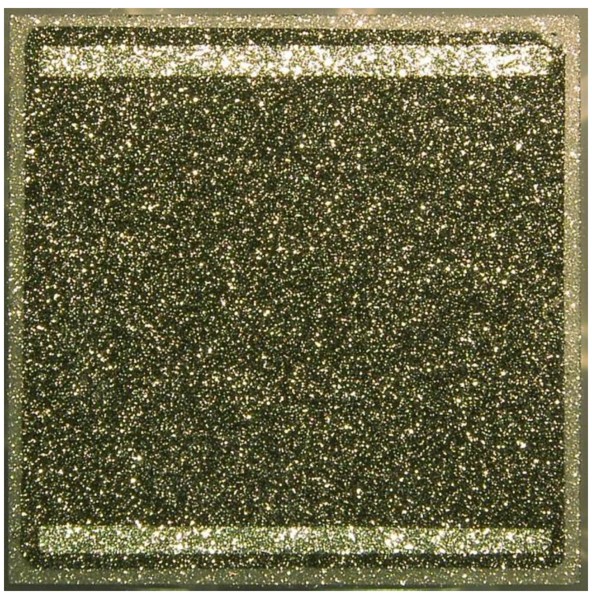

growth side

The U – I characteristic (meas. @GSI)

Recent tests: DD2

LACPSDD polycrystalline-Element 6: electronic grade, **10 mm x 10 mm**, =110μm, 2 DLC layers **(Dr. Michal Pomorski)**, electrodes and bonding (**GSI**)

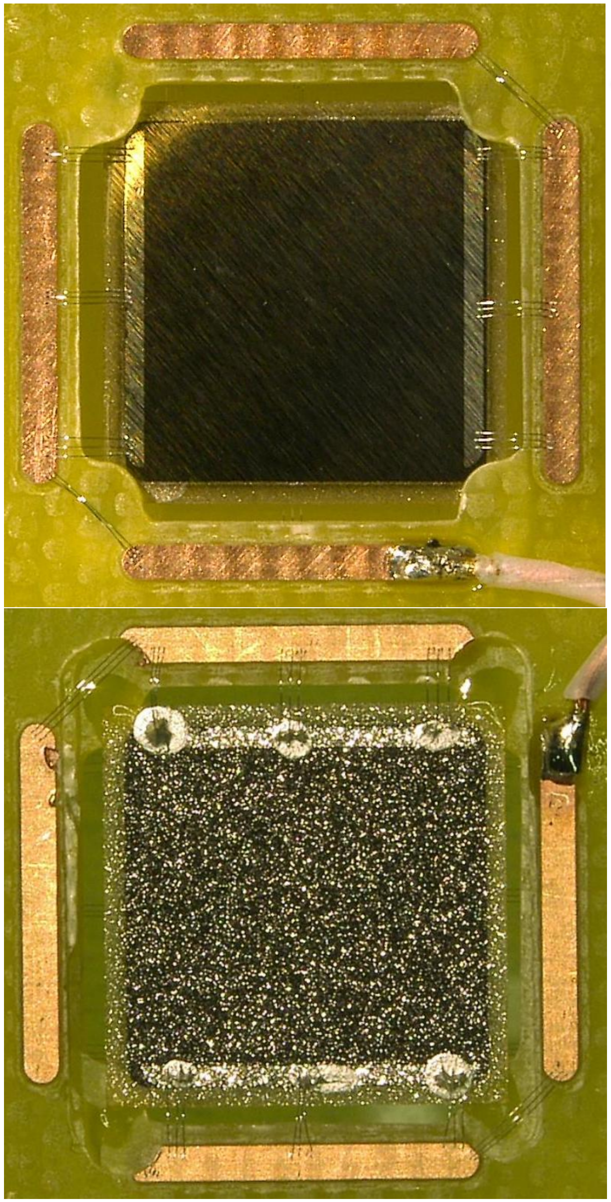

substrate side

RD=7 - 38 KΩ□

growth side: strip-strip R=37.9kOhm +/-0.2kOhm

substrate side: strip-strip R=7.04kOhm +/-0.2kOhm

CD= 49.5pF

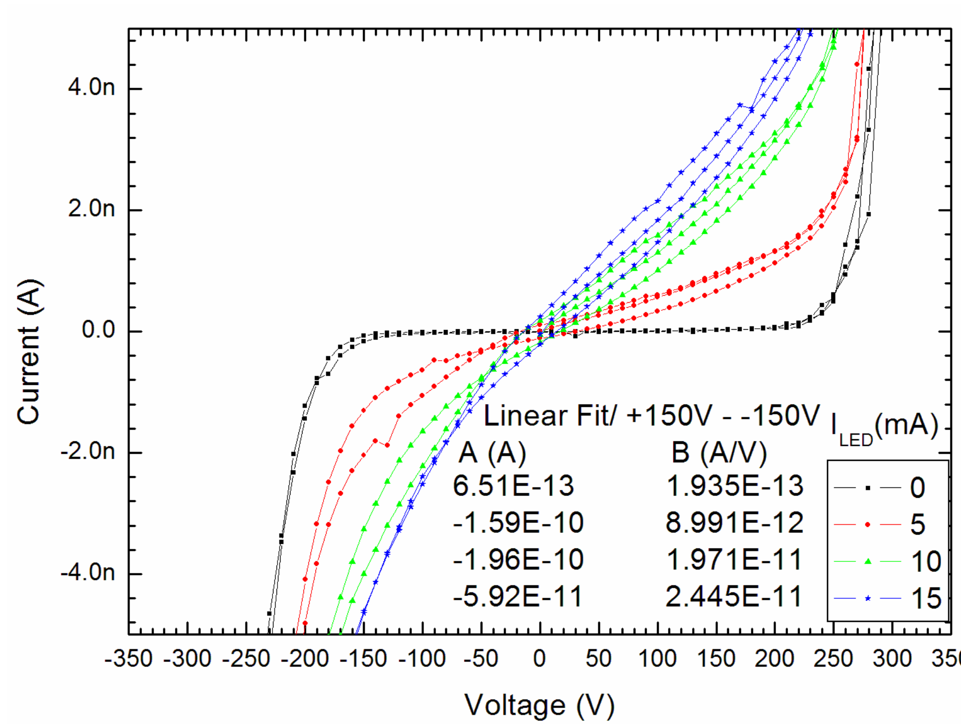

growth side

The U – I characteristic (meas. @ISS)

Tests with Alpha, DD1 and DD2

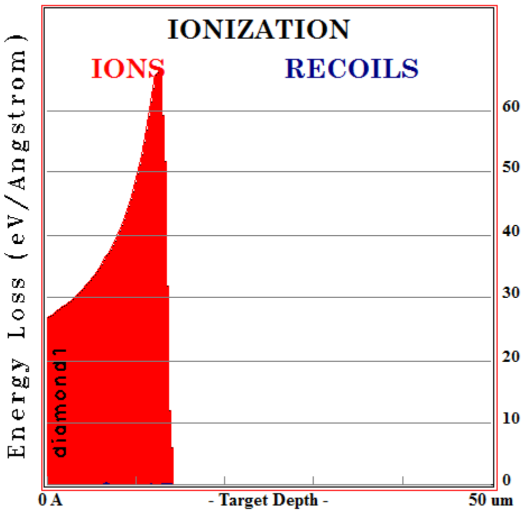

Am 241 E_{Alpha}=5.486 MeV
(Q_{Alpha}~ 67 fC)

- Noise: APFEL and TCSA1 have (on used detector capacitance) σ_N=0.6fC rms; +/- 3 σ_N ~ 4 fC pp
- S/N = 33.5/4 ~ 8, for two channels connected to the same 67 fC charge

1) Tests with APFEL chip front-end DD2

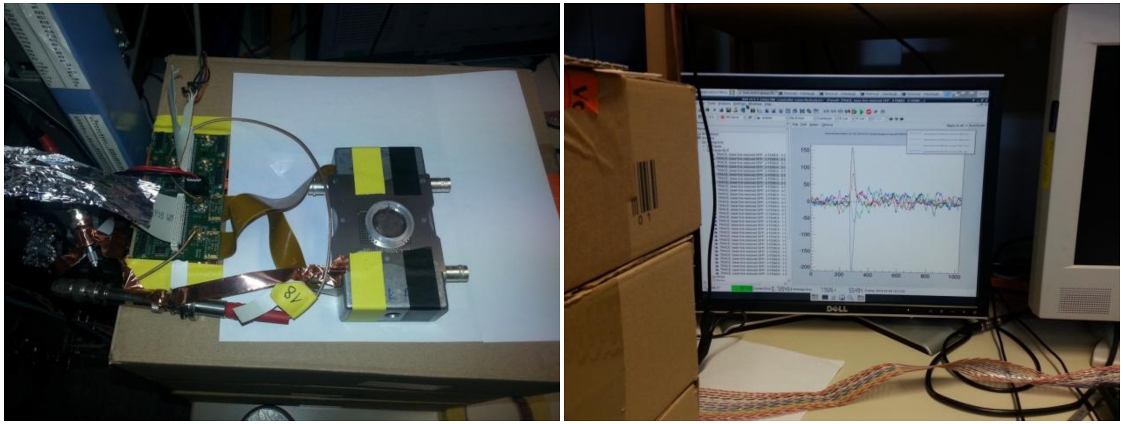

2) Tests with TCSA1 front-end DD1 and DD2

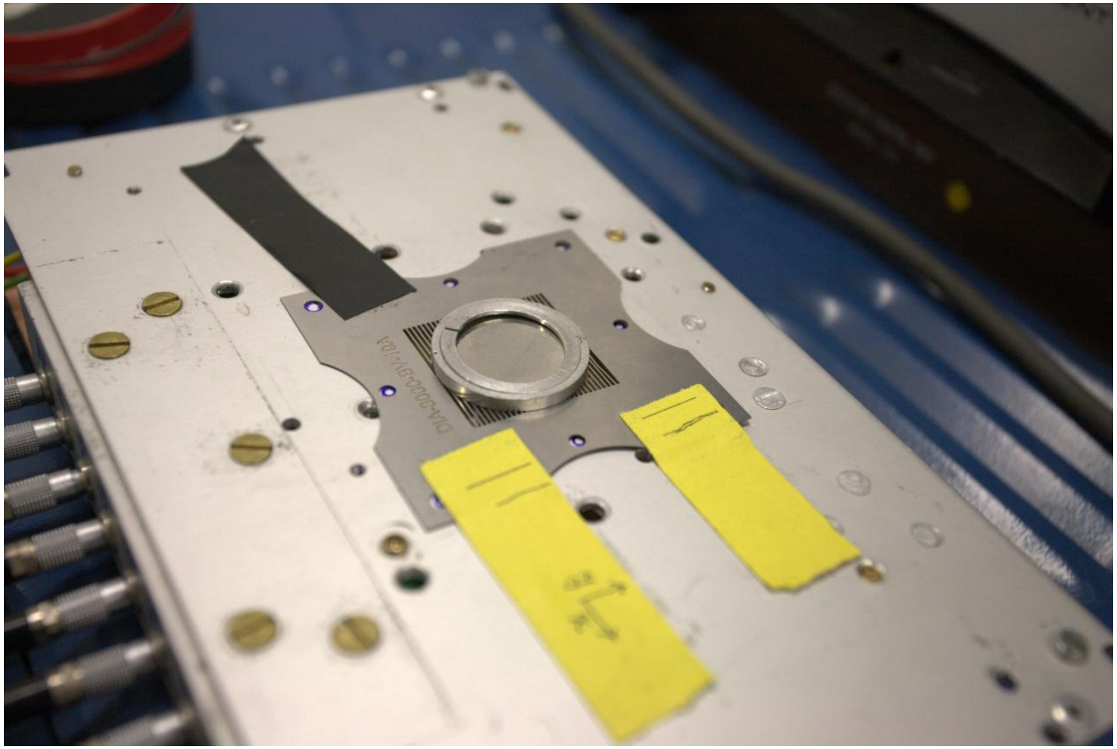

Tests with Alpha, DD2: 1) APFEL 1_3 ASIC chip front-end

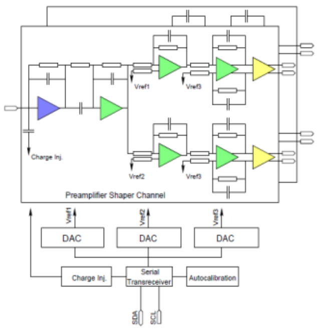

Figure 5. The readout concept of the ASIC consists of an analog readout chain ai digital part allows to set different reference voltages to operate in a wide temperatu dynamic range.

Gain of		
signal path 1:	10.41 ± 0.069	mV/fC
signal path 2:	0.332 ± 0.055	mV/fC
Peaking time:	248 ± 3	ns
ENC:	0.62 ± 0.03	fC
Max. input charge:	6.31	pC
Dynamic range:	10 052	1
Power consumption:	56.5±0.5	mW/Channel

Table 2. Summary of the measurement results at T=-20°C.

H. Flemming and P. Wieczorec, Low Noise Preamplifier ASIC for PANDA Experiment

The four currents pulse height spectrum

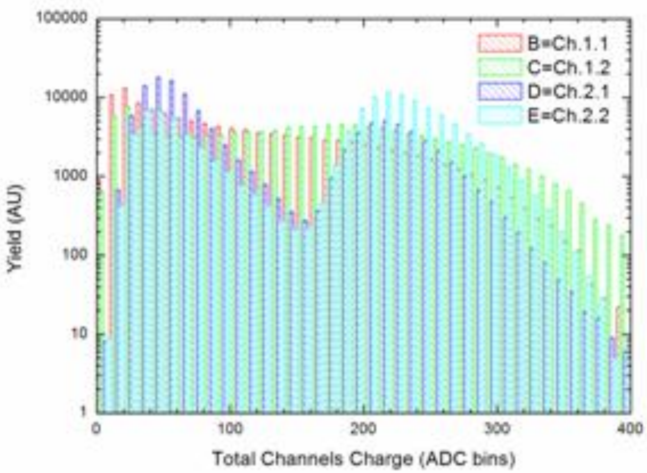

The two layers total currents PH spectrum

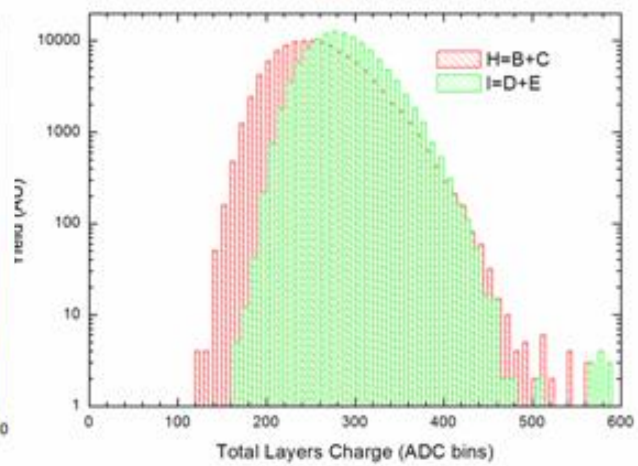

The two layers currents ratio spectrum

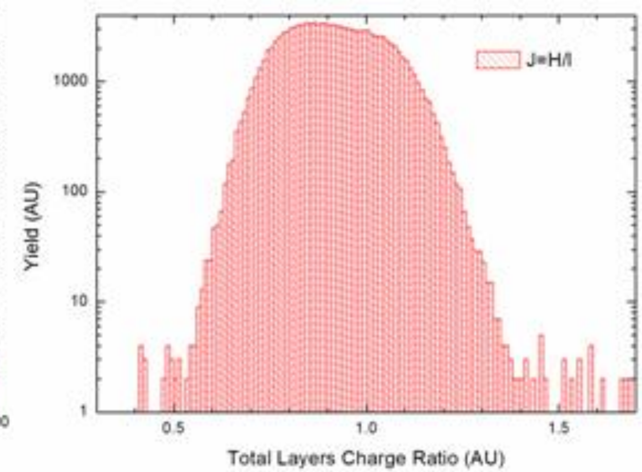

The different surface resistivity of DLC layers generates a non uniform response. The structure seen in pulse height spectrum is more pronounced for the high resistivity layer which suggests a ballistic deficit in front-end electronics.

Tests with Alpha, DD2: 1) APFEL 1_3 ASIC chip front-end

Holes and electrons current scatter

Position reconstruction

Signal pick value

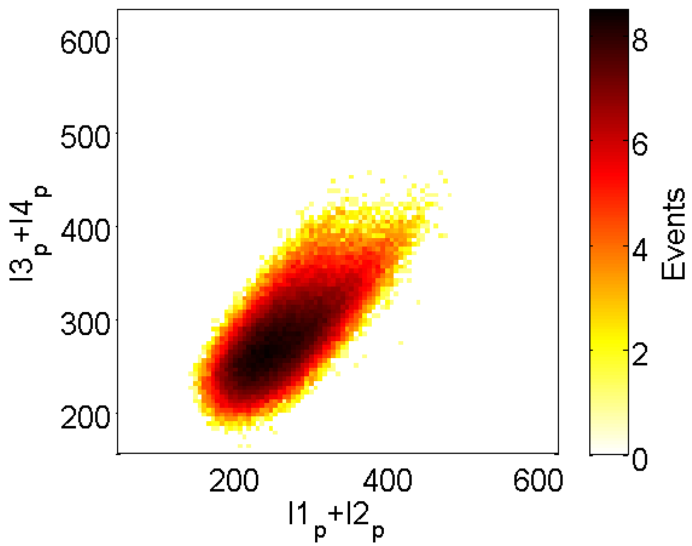

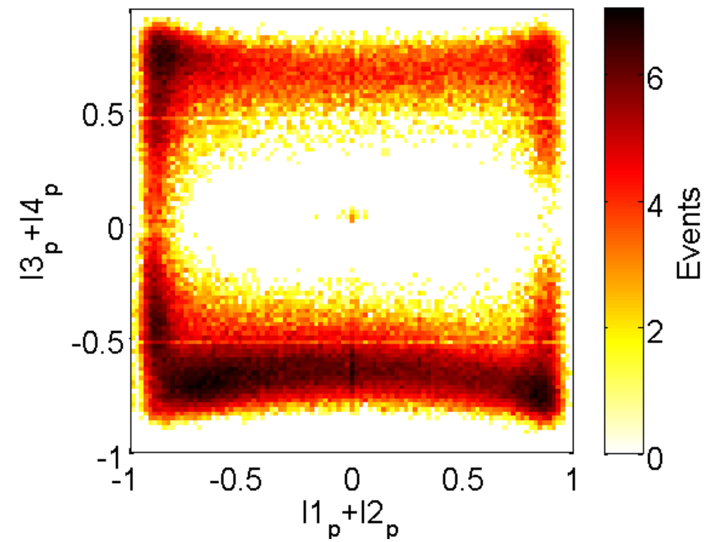

Signal integral value

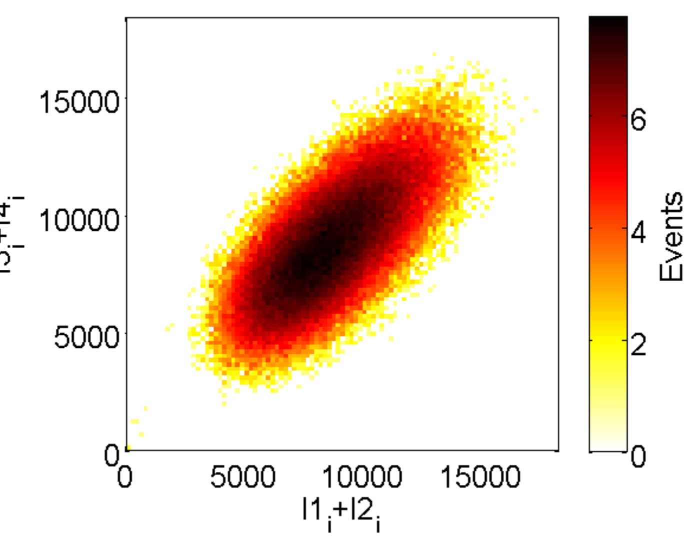

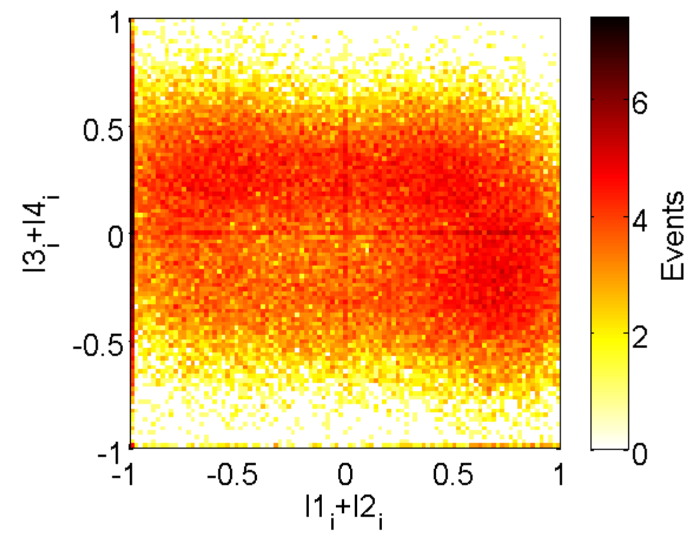

Conclusion: The picking time of CSA must be bigger to avoid ballistic deficit!

Tests with Alpha, DD1:
2) TCSA1 front-end, modified to have 1.5μs peacking time

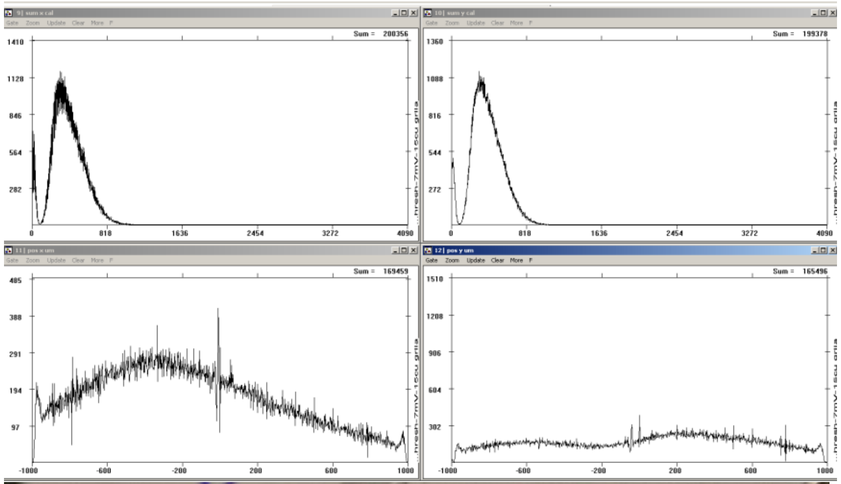

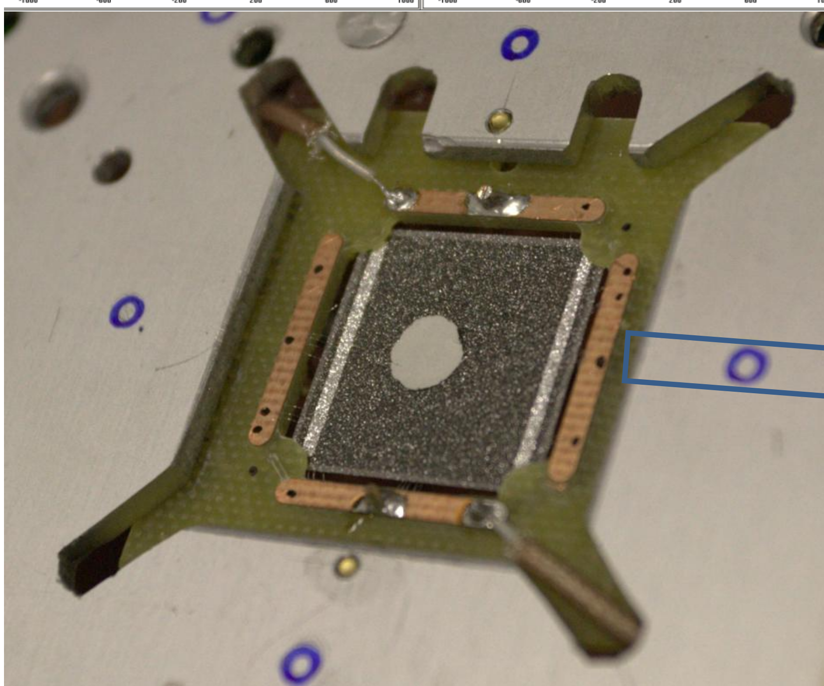

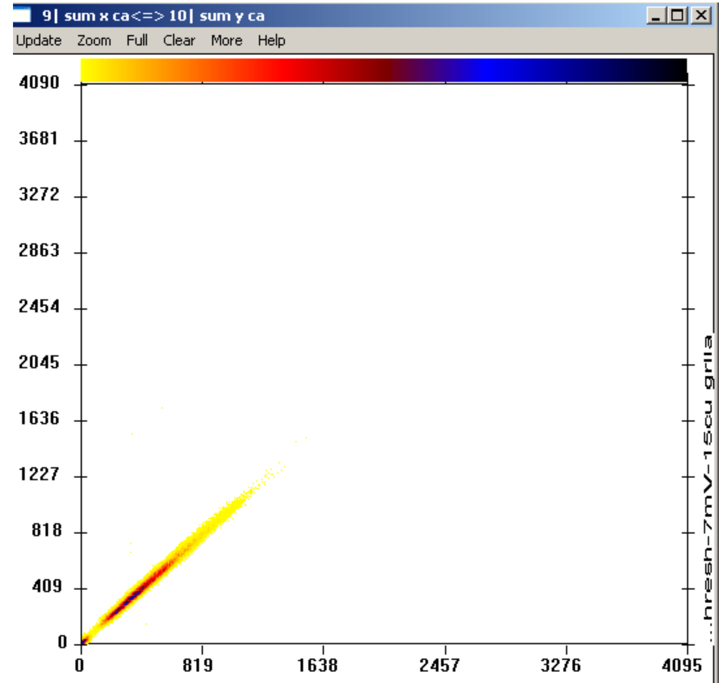

?

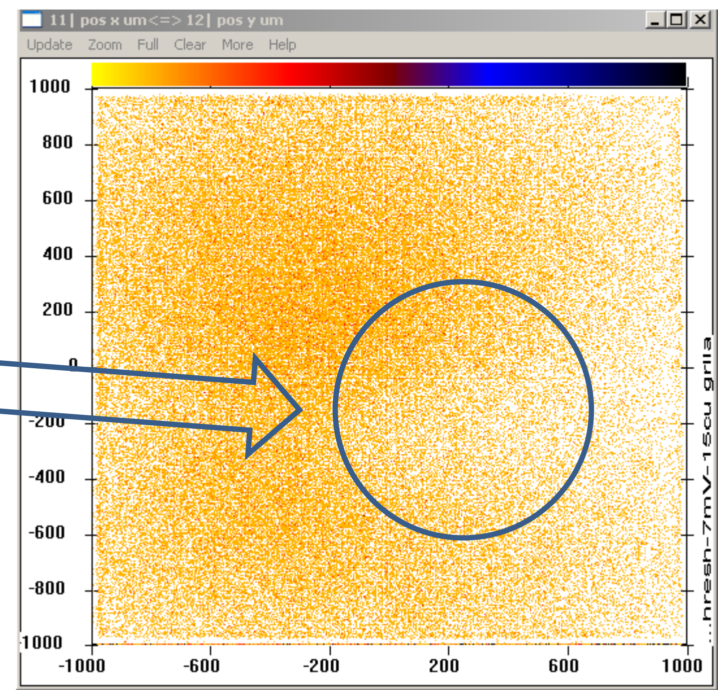

Tests with Alpha, DD2: More about the Signal to Noise importance in position reconstruction applications

$$X = \frac{Q_1 - Q_2}{Q_1 + Q_2} \cdot \frac{L}{2} \quad ; \quad Y = \frac{Q_3 - Q_4}{Q_3 + Q_4} \cdot \frac{L}{2}.$$

Q_i are the charges measured by the collecting electrodes of the two resistive DLC layers.

$$U_i = G_{Ci} \cdot Q_i + U_{Ni} = U_{Si} + U_{Ni} = U_{Si} \cdot (1 + \frac{U_{Ni}}{U_{Si}}) = U_{Si} \cdot (1 + N_i / S_i) \, .$$

where G_{Ci} is the conversion gain, U_{Ni} is the noise, and S/N_i^{-1} is the inverse of the signal to noise ratio of the cell *i*.

If we note: $U_{S1}+U_{S2}=U_S$, $U_{S1}=kU_S$ and $U_{S2}= (1-k)U_S$,

$$X = \frac{U_1 - U_2}{U_1 + U_2} \cdot \frac{L}{2}$$

$$X = \frac{U_{S1}(1 + N_1/S_1) - U_{S2}(1 + N_2/S_2)}{U_{S1}(1 + N_1/S_1) + U_{S2}(1 + N_2/S_2)} \cdot \frac{L}{2};$$

$$X = \left[\frac{2 \cdot k - 1 + k \cdot N_1/S_1 - (1-k) \cdot N_2/S_2}{1 + k \cdot N_1/S_1 + (1-k) \cdot N_2/S_2} \right] \cdot \frac{L}{2};$$

Similarly, if we introduced *l* instead of *k* for *Y* axis, .

$$Y = \frac{U_3 - U_4}{U_3 + U_4} \cdot \frac{L}{2}$$

$$Y = \left[\frac{2 \cdot l - 1 + l \cdot N_3/S_3 - (1-l) \cdot N_4/S_4}{1 + l \cdot N_3/S_3 + (1-l) \cdot N_4/S_4} \right] \cdot \frac{L}{2}.$$

In addition, resistively coupled CSA presents a correlated noise; in our case (big detector capacitance) this noise component is relatively small (~ 20%).

S. P. Bönisch, B. Namaschk, F. Wulf, Charge equalizing and error estimation in position sensitive neutron detectors, *NIM A 570 (2007) 133-139*

S. P. Bönisch, B. Namaschk, F. Wulf, Low-Frequency Noise of Resistively Coupled Charge Amplifiers *IEEE TNS, VOL. 55, NO. 4, AUGUST 2008*

^{12}C microbeam tests, DD1

E_{Beam}=11.4 MeV/A

The energy loss for stopped particles is ~25 times bigger then in the alpha case.

For DD2, 10mm x 10mm, 110µm thick, there are traversing ions.

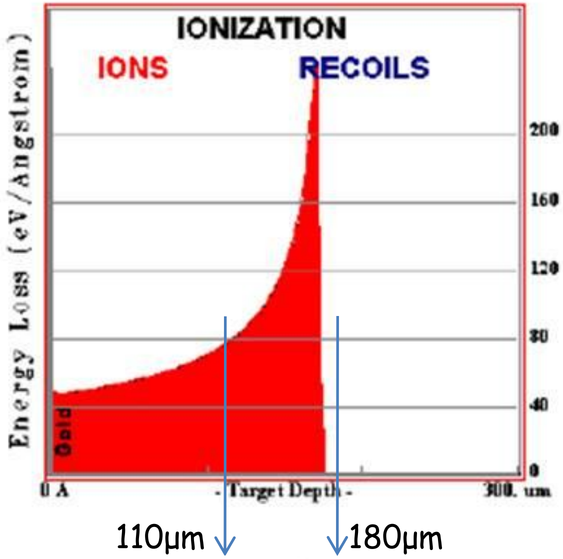

For DD1, 20mm x 20mm, 180µm thick, there are stopped ions.

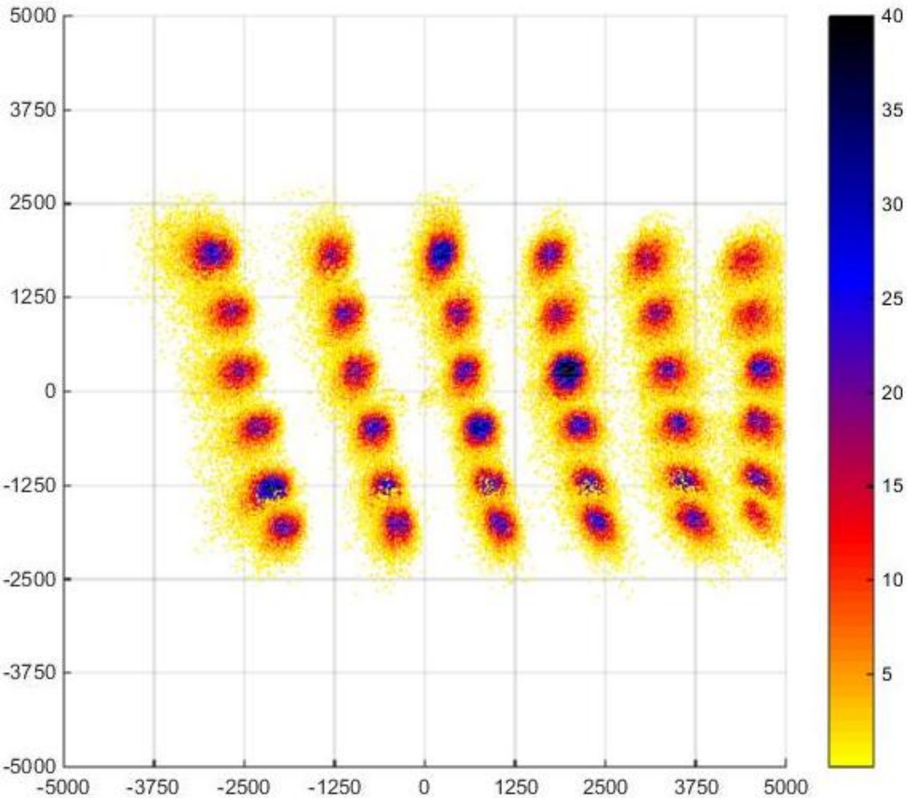

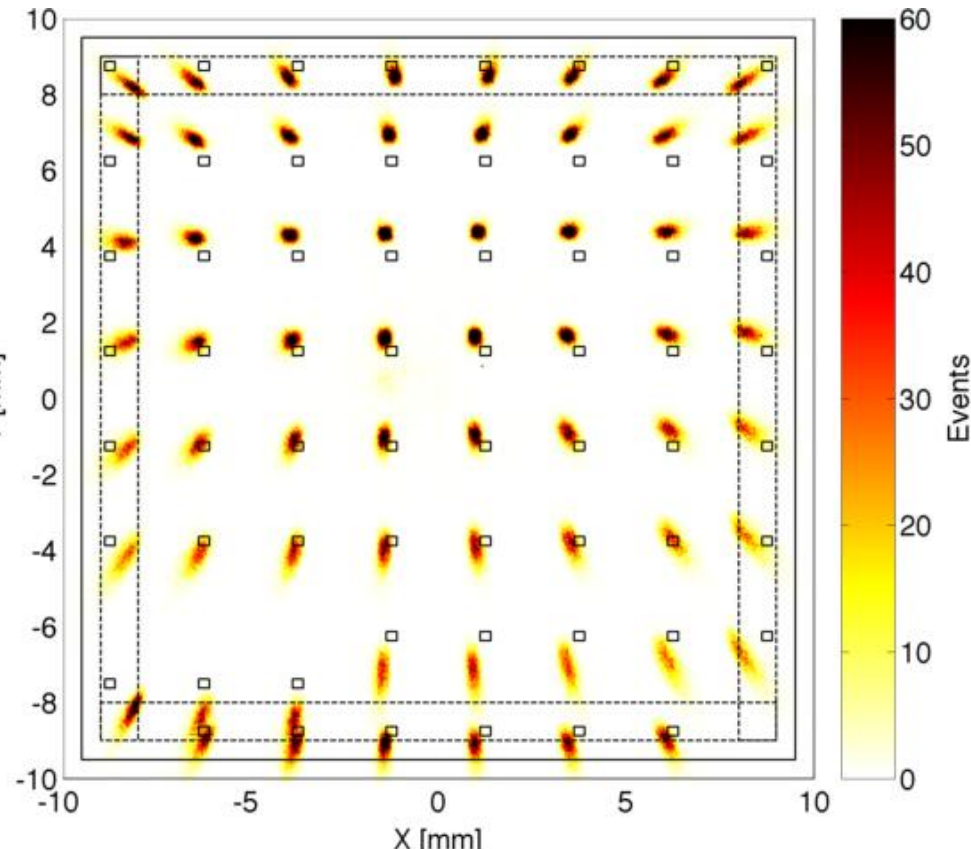

Microbeam tests, DD1: Data filtering and position fitting

a)

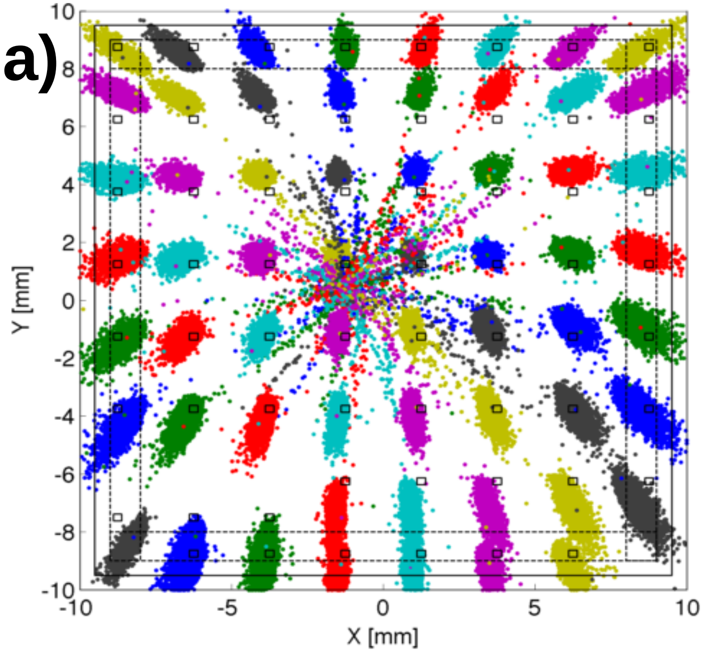

a) Initial data, corresponding to the 64 microbeam positions. Each color is associated with one position ('frame').

b) The median center (x,y), the median absolute deviation ($MAD_{x,y}$), and the standard deviation, approximated by $\sigma_{x,y}=1.4826 * MAD_{x,y}$ (valid for a normal distribution), are computed for each frame. Events outside the Center +/-4 $\sigma_{x,y}$ and outside collecting strips area (a total of a few percent) are ignored.

c) The remaining point are fitted to gaussian 2D distributions, providing higher accuracy estimates of the Centers.

b)

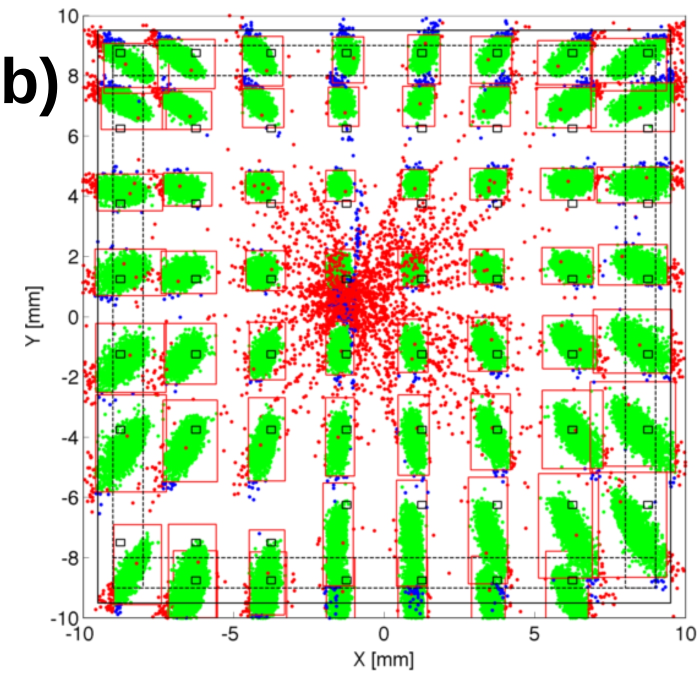

c)

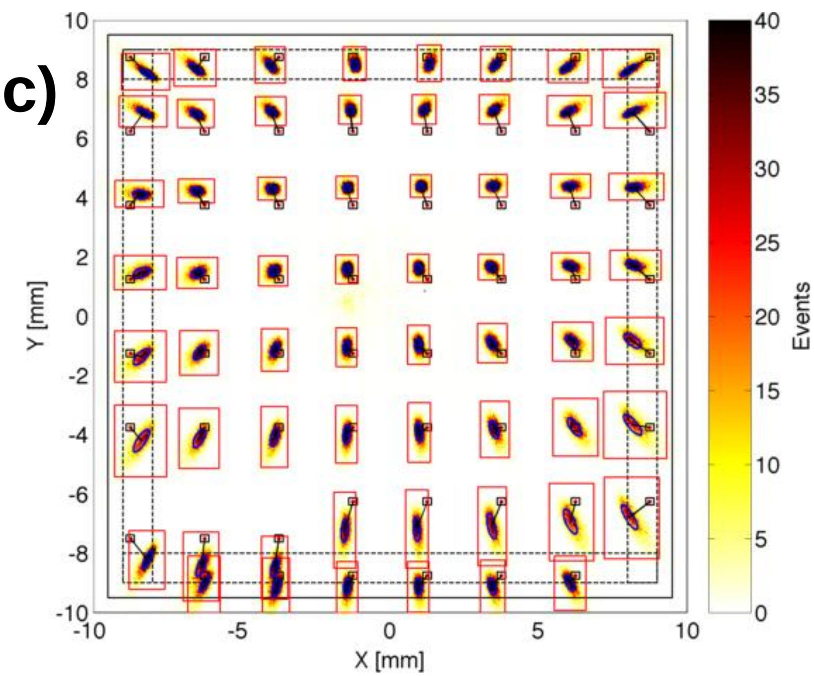

Microbeam tests, DD1: Fitting of the reconstruction errors

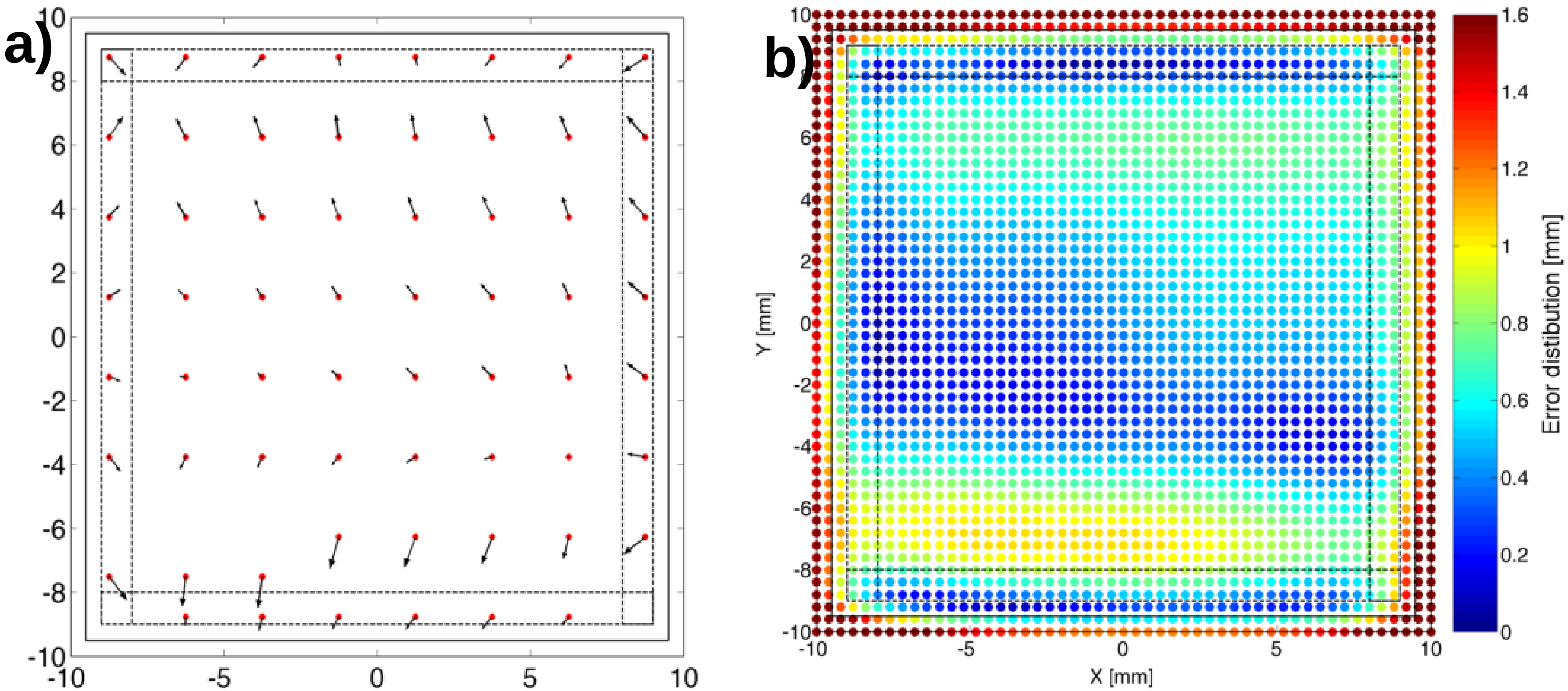

a) For each of the 64 microbeam positions, an error vector is computed, based on the known microbeam focus and on the fitted actual position.

b) The x and y components of the error vectors are fitted by series expansions of 2D Legendre polynomials. Under nominal operation, this derived 'calibration function' is meant to correct the measured data and provide increased accuracy of position reconstruction.

Microbeam tests, DD1: Fitting of the reconstruction errors

c)

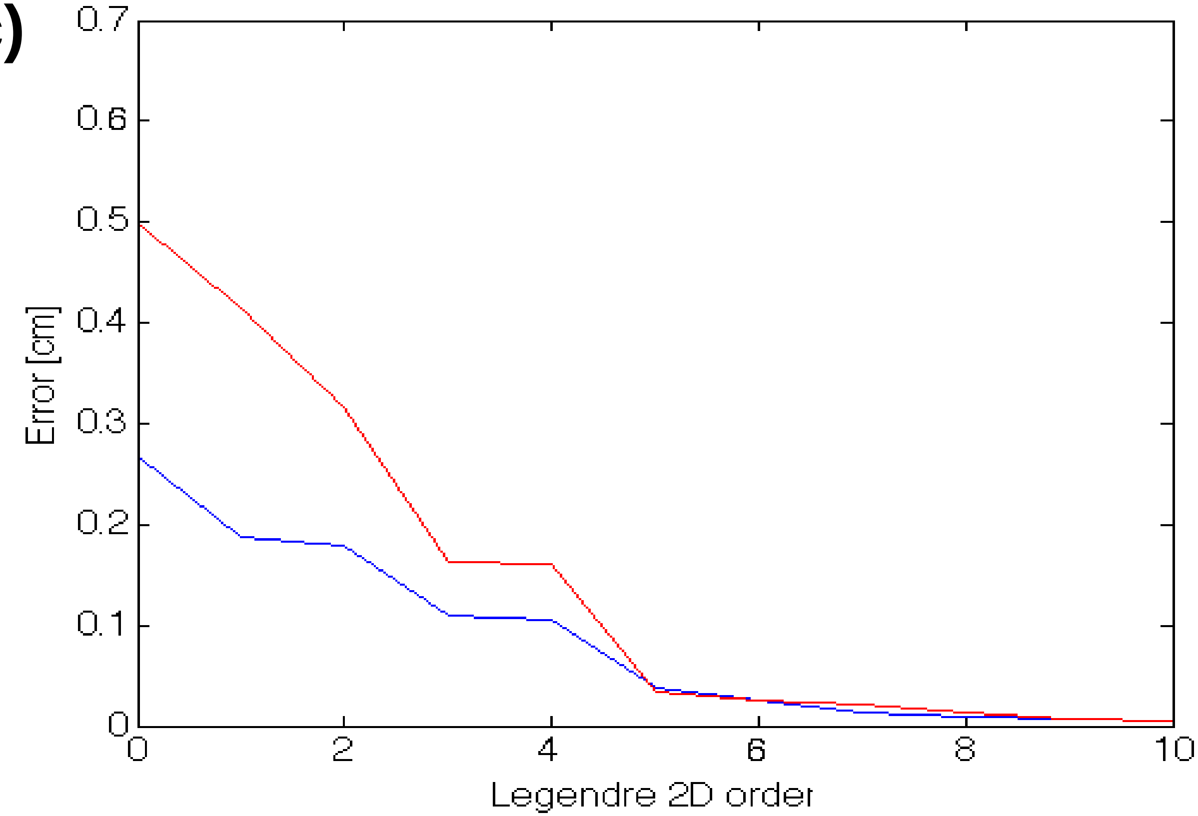

c) The degree of the series expansion is derived self consistently, by computing the residual beteen the respective components of the error vectors depending on the expansion degree. In our case, this dependence becomes rather flat for $n \geq 5$, i.e. the minimum required degree is 5.

In addition, the residuals for both x and y components become equal at n=5, supporting the expected small scale isotropy of the detector (not affected by e.g. electrical biases, which can influence lower order expansions).

Microbeam tests, DD1: Cross-check of the fitted reconstruction errors

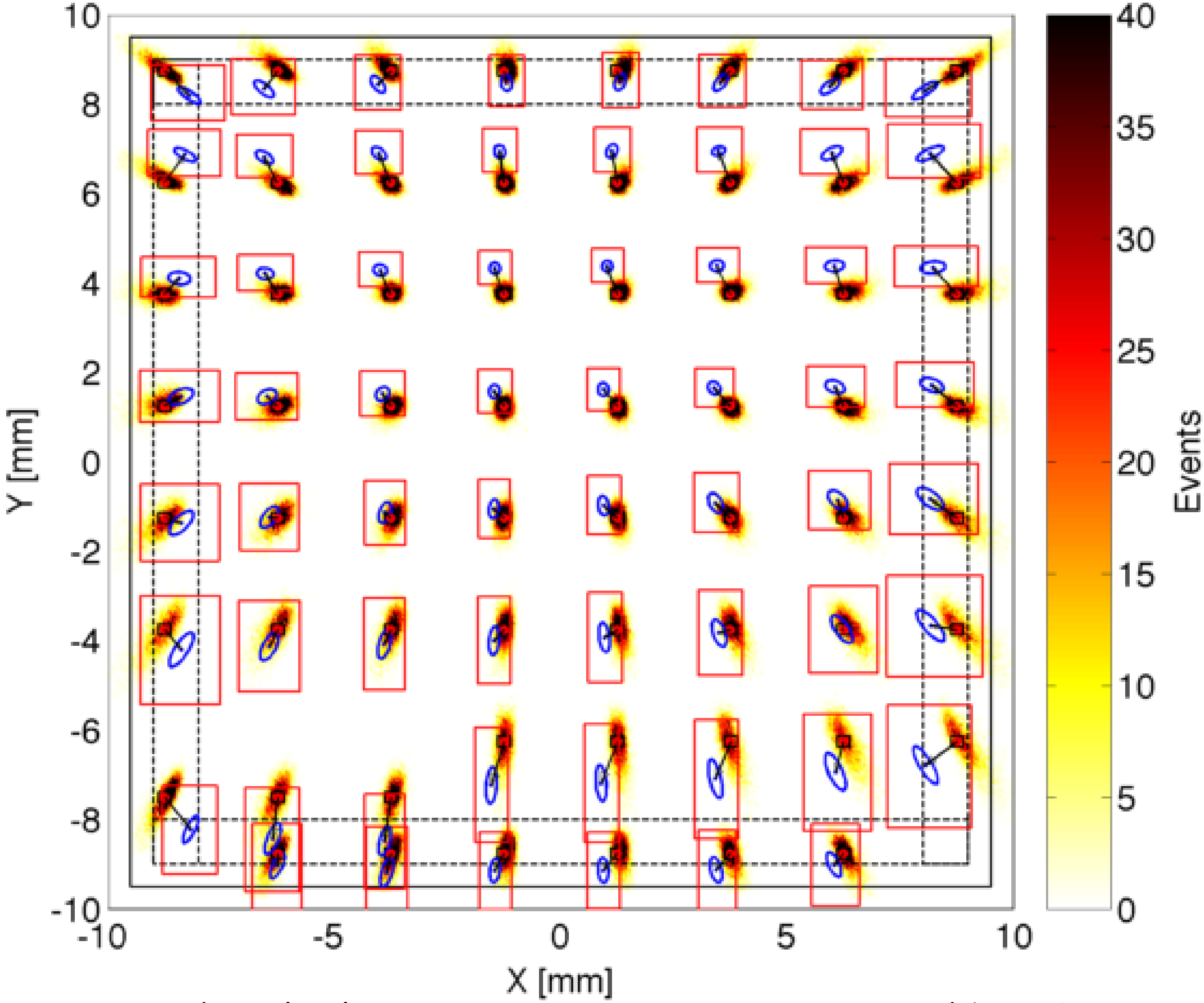

When corrected with the error vectors approximated by 2D Legendre polynomials, the 64 measured distributions agree fairly well with the microbeam injection frames.

Improved configuration

We propose a new structure for the collecting electrodes and FEE.

We add 4 supplementary strips on each axis, to reduce 5 times the S/N dynamics. We increase from 4 to 12 the CSA number.

The new structure: simulation with distributed elements layout (COMSOL).

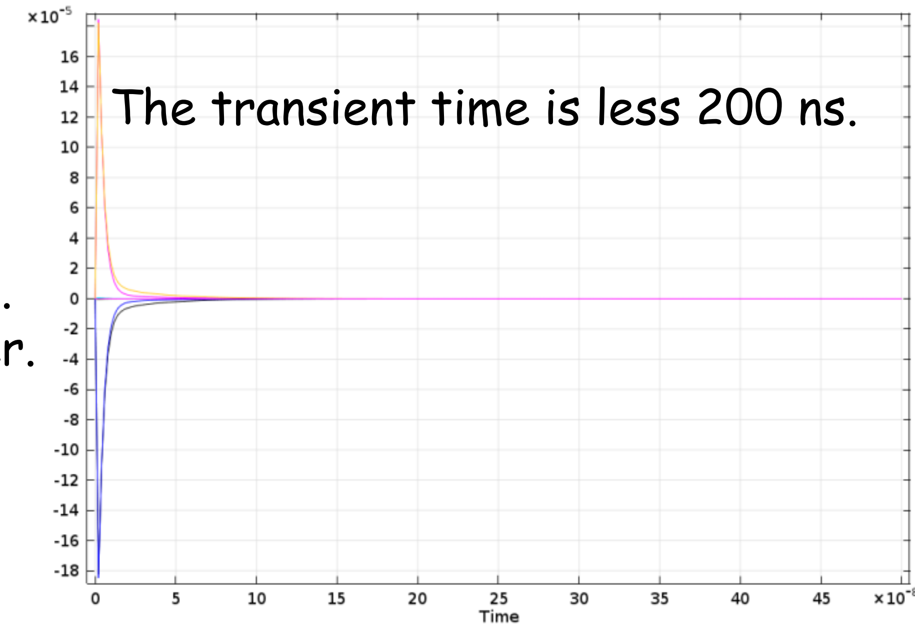

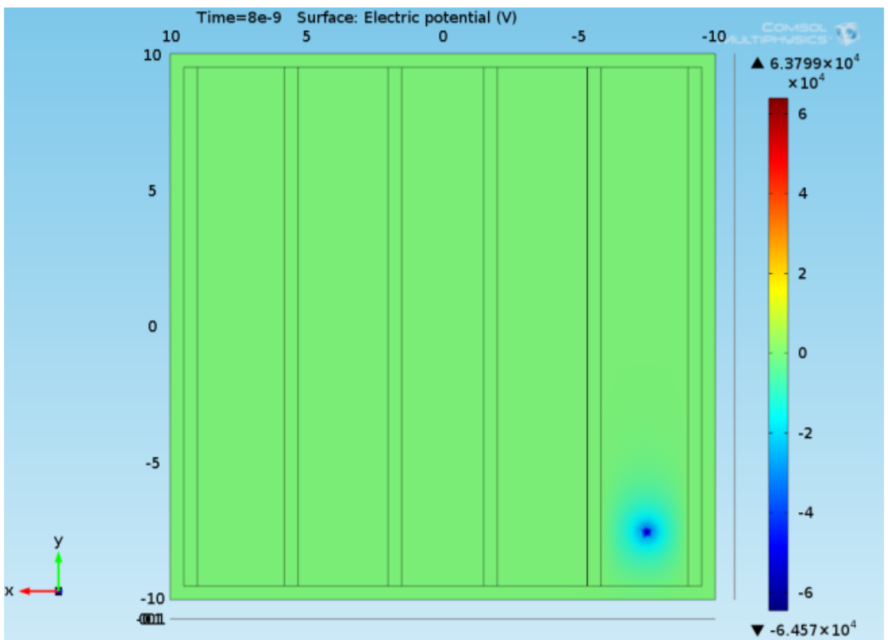

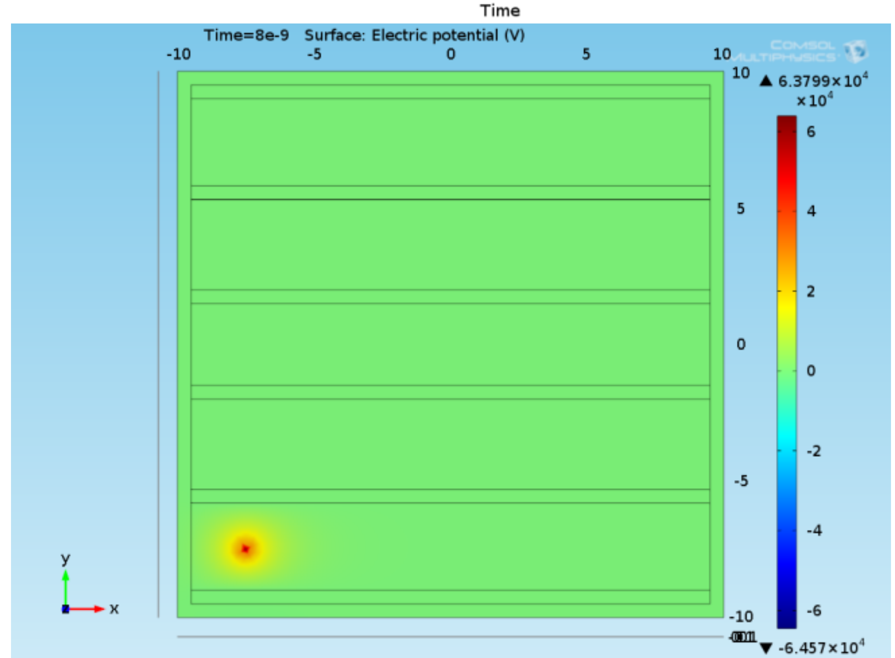

Improved configuration

Simulation with concentrated elements schematics
(APLAC).

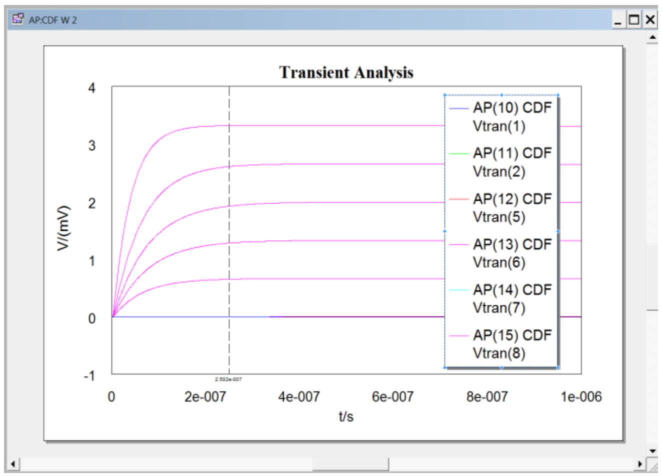

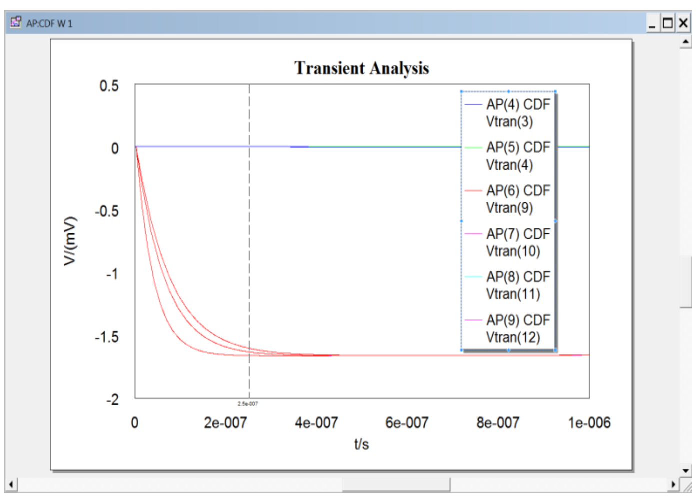

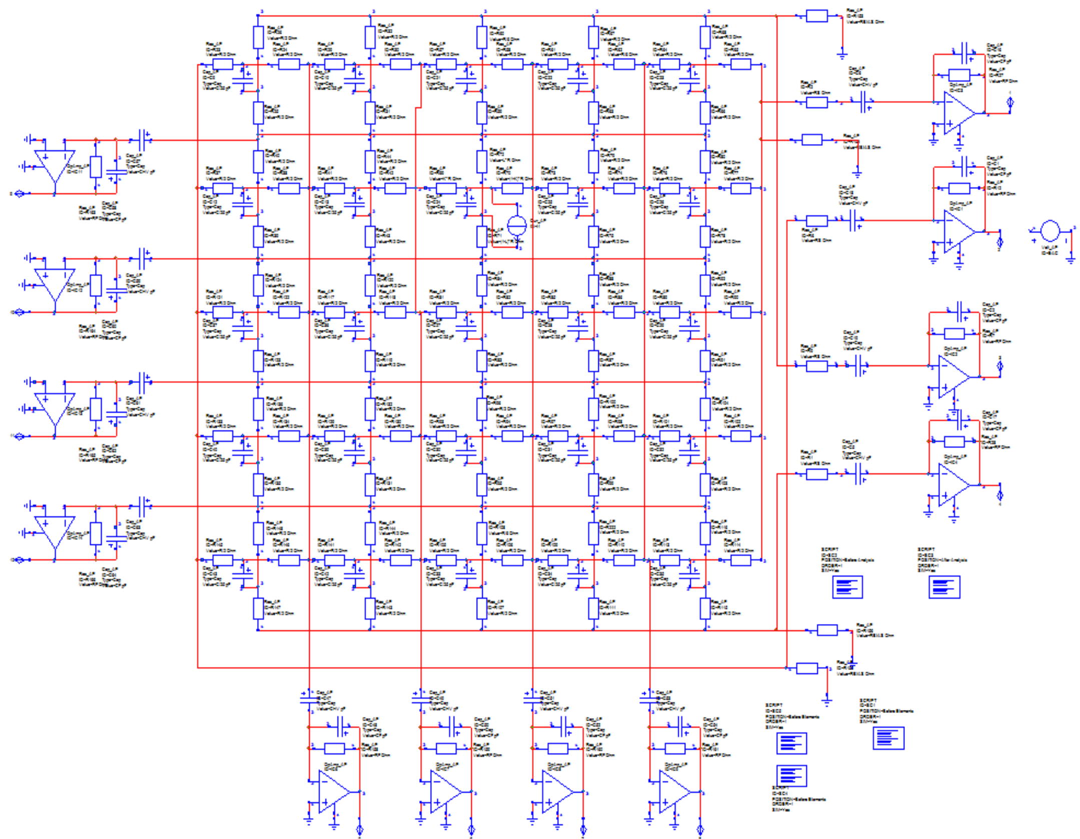

The transient time less 200 ns.

Summary

- We understood the main errors made in the 2012 test:
  1. The very high rate of events related to CAMDA-CAMAC data acquisition system.
  2. The FEE picking time not matched with the Detector time constant.
- We made tests with Alpha and ^{12}C to improve the measurement accuracy.
- The LACPSDD concept has been proved: it works!

Outlook

- The main limitations are related to:
  1. The pc material has a large dynamics of the induced signal which affects the S/N.
  2. The Detector time constant.
  3. The CSA noise.
- We propose a new detector structure, which decreases the detector time constant and the S/N dynamics.
- We think that the change to DoI material will extend the area of applicability.

People:

-CEA-Saclay: M.Pomorski

-GSI-Darmstadt: E.Berdermann, M.Kis, M.Traeger, K-O.Voss, P.Wieczorek

-ISS-Bucharest: C.Bunescu, M.Ciobanu, H.Comisel, V.Constantinescu, O.Marghitu

Acknowledgment:

ISS-Bucharest: - Romanian Space Agency through STAR programme, DIADEMS project.
- ADAMAS collaboration

The Reconstruction Error estimation

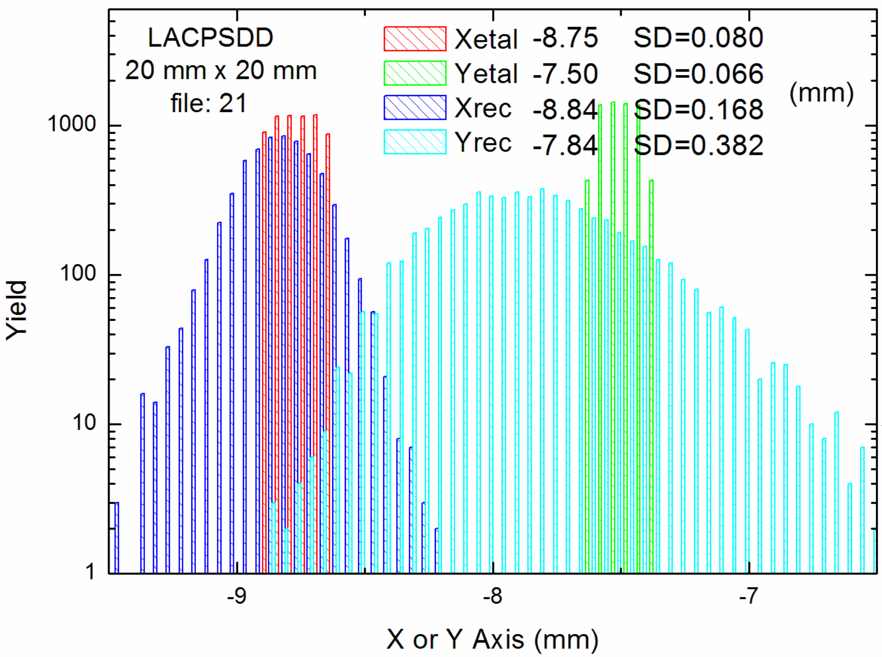

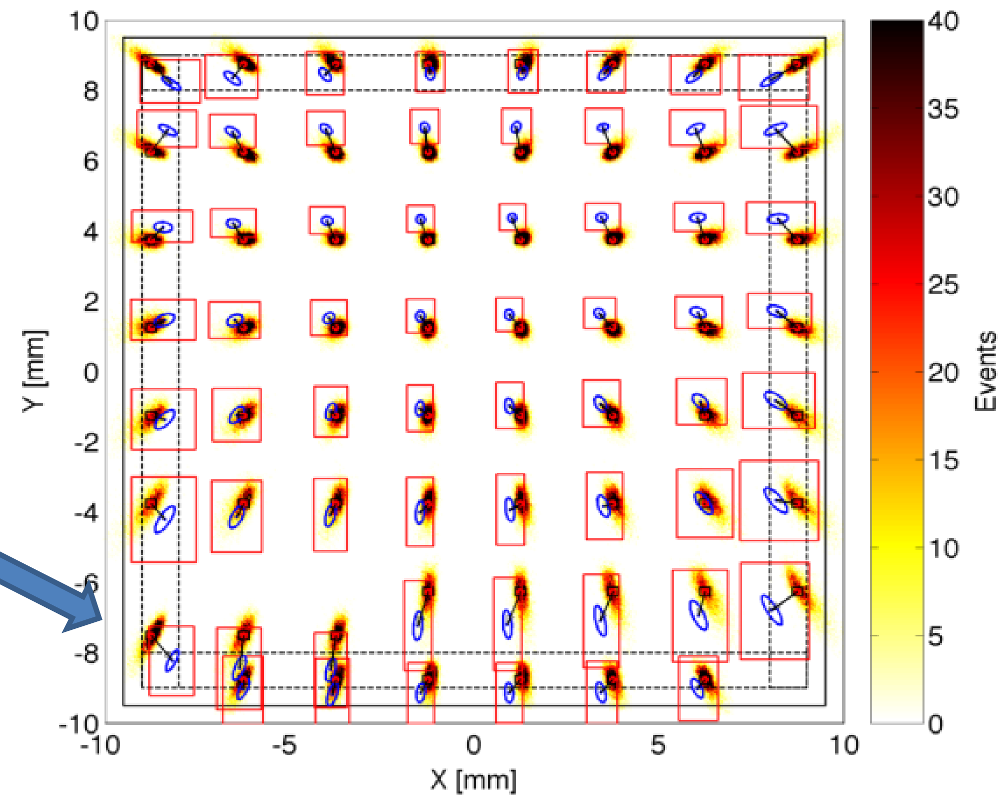

The mean RMS error:

$$Gerror_x(cadru) = \frac{1}{\sqrt{N\_cadru}} \sqrt{\sum_{1}^{N\_cadru} (x\_abs - x\_comp)^2}$$

$$Gerror_y(cadru) = \frac{1}{\sqrt{N\_cadru}} \sqrt{\sum_{1}^{N\_cadru} (y\_abs - y\_comp)^2}$$

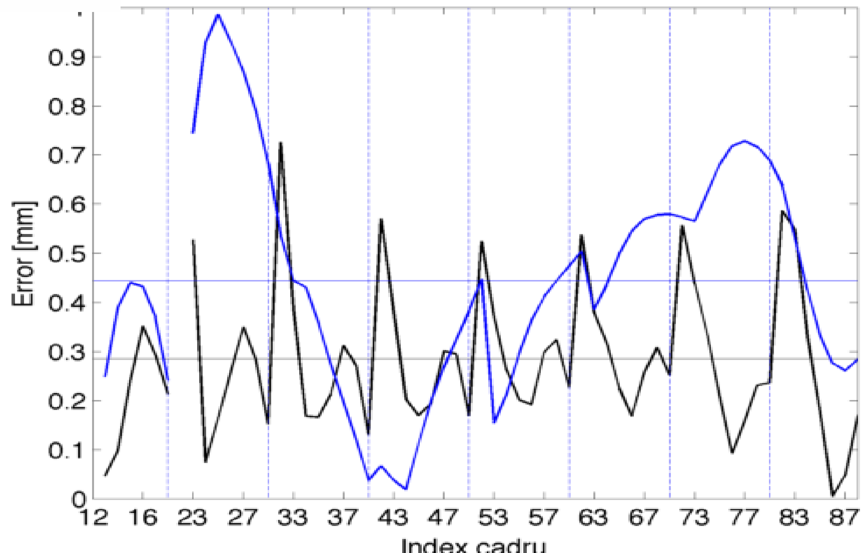

0.44 mm

0.28 mm